World Journal of Gastroenterology

Submit a Manuscript: https://www.f6publishing.com

World J Gastroenterol 2023 May 28; 29(20): 3103-3118

DOI: 10.3748/wjg.v29.i20.3103

ISSN 1007-9327 (print) ISSN 2219-2840 (online)

ORIGINAL ARTICLE

Basic Study

Dihydroergotamine ameliorates liver fibrosis by targeting transforming growth factor β type II receptor

Ke-Xin Zheng, Shou-Li Yuan, Meng Dong, Han-Lin Zhang, Xiao-Xiao Jiang, Chun-Long Yan, Rong-Cai Ye, Hui-Qiao Zhou, Li Chen, Rui Jiang, Zi-Yu Cheng, Zhi Zhang, Qi Wang, Wan-Zhu Jin, Wen Xie

Specialty type: Gastroenterology and hepatology

Provenance and peer review: Unsolicited article; Externally peer reviewed.

Peer-review model: Single blind

Peer-review report's scientific quality classification

Grade A (Excellent): 0
Grade B (Very good): B, B
Grade C (Good): 0
Grade D (Fair): 0
Grade E (Poor): 0

P-Reviewer: Jena MK, India; Shrewsbury SB, United States

Received: February 6, 2023
Peer-review started: February 6, 2023
First decision: March 21, 2023
Revised: April 1, 2023
Accepted: April 24, 2023
Article in press: April 24, 2023
Published online: May 28, 2023

Ke-Xin Zheng, Qi Wang, Wen Xie, Center of Liver Diseases, Beijing Ditan Hospital, Capital Medical University, Beijing 100015, China

Shou-Li Yuan, Meng Dong, Han-Lin Zhang, Xiao-Xiao Jiang, Chun-Long Yan, Rong-Cai Ye, Hui-Qiao Zhou, Li Chen, Rui Jiang, Zi-Yu Cheng, Zhi Zhang, Wan-Zhu Jin, Key Laboratory of Animal Ecology and Conservation Biology, Institute of Zoology, Chinese Academy of Sciences, Beijing 100101, China

Shou-Li Yuan, Han-Lin Zhang, Xiao-Xiao Jiang, Rong-Cai Ye, Hui-Qiao Zhou, Li Chen, Rui Jiang, Zi-Yu Cheng, Zhi Zhang, Graduate School, University of the Chinese Academy of Sciences, Beijing 100049, China

Chun-Long Yan, Graduate School, Agriculture College of Yanbian University, Yanji 133002, Jilin Province, China

Corresponding author: Wen Xie, MD, Doctor, Center of Liver Diseases, Beijing Ditan Hospital, Capital Medical University, No. 8 Jingshun East Street, Chaoyang District, Beijing 100015, China. xiewen6218@163.com

Abstract

BACKGROUND

The transforming growth factor β (TGFβ) signaling pathway plays a crucial role in the development of liver fibrosis by activating TGFβ type II receptor (TGFβR2), followed by the recruitment of TGFβR1 finally triggering downstream signaling pathway.

AIM

To find drugs targeting TGFβR2 that inhibit TGFβR1/TGFβR2 complex formation, theoretically inhibit TGFβ signaling pathway, and thereby ameliorate liver fibrosis.

METHODS

Food and Drug Administration-approved drugs were screened for binding affinity with TGFβR2 by virtual molecular docking. We identified 6 candidates and further explored their potential by Cell Counting Kit-8 (CCK-8) cell cytotoxic experiment to validate toxicity and titrated the best cellular working concentrations. Next, we further demonstrated the detailed molecular working

mechanisms using mutagenesis analysis. Finally, we used a mouse model to investigate its potential anti-liver fibrosis effect.

RESULTS

We identified 6 drug candidates. Among these 6 drugs, dihydroergotamine (DHE) shows great ability in reducing fibrotic gene expressions such as collagen, p-SMAD3, and α-SMA in TGFβ induced cellular model of liver fibrosis in LX-2 cells. Furthermore, we demonstrated that DHE binds to TGFβR2. Moreover, mutation of Leu27, Phe30, Thr51, Ser52, Ile53, and Glu55 of TGFβR2 disrupted the binding of TGFβR2 with DHE. In addition, DHE significantly improved liver fibrosis, as evidenced by Masson's trichrome staining of liver sections. This is further supported by the width and the velocity of the portal vein, and serum markers of liver function. In line with those observations, DHE also decreased macrophages infiltration and extracellular matrix deposition in the liver.

CONCLUSION

DHE alleviates liver fibrosis by binding to TGFβR2 thereby suppressing TGFβ signaling pathway. We show here that as far as drug repurposing, DHE has great potential to treat liver fibrosis.

Key Words: Liver fibrosis; Transforming growth factor β (TGFβ) signaling pathway; TGFβ type II receptor (TGFβR2); Virtual screening; Drug-repurposing; Dihydroergotamine

Core Tip: An effective and safe drug for treating liver fibrosis is urgently needed in current clinical practice. Here, we investigated and discovered that dihydroergotamine (DHE) could alleviate liver fibrosis by specific binding of transforming growth factor β type II receptor (TGFβR2) to disrupt the binding of TGFβR2 with TGFβ1, and ultimately suppressing its downstream TGFβ signaling pathway. DHE may be an effective anti-liver fibrosis drug, which could be employed in liver cirrhotic patients.

Citation: Zheng KX, Yuan SL, Dong M, Zhang HL, Jiang XX, Yan CL, Ye RC, Zhou HQ, Chen L, Jiang R, Cheng ZY, Zhang Z, Wang Q, Jin WZ, Xie W. Dihydroergotamine ameliorates liver fibrosis by targeting transforming growth factor β type II receptor. *World J Gastroenterol* 2023; 29(20): 3103-3118
URL: https://www.wjgnet.com/1007-9327/full/v29/i20/3103.htm
DOI: https://dx.doi.org/10.3748/wjg.v29.i20.3103

INTRODUCTION

Liver fibrosis is the consequence of various chronic pathogenic factors[1], it is a dynamic process that is characterized by an excessive accumulation of extracellular matrix[2]. Early liver fibrosis can be reversed to a normal architecture by removal of underlying causes[2], but liver fibrosis could further develop into cirrhosis without effective treatment[3]. Liver cirrhosis can be complicated by variceal bleeding, hepatic encephalopathy, ascites, bacterial peritonitis, and hepatocellular carcinoma, which has high mortality[4]. Liver cirrhosis can regress to early stage of disease, but it cannot be reversed to a normal liver[5]. Therefore, it is very important to control the disease progression in the early reversible stage of liver fibrosis.

Etiological treatment of liver fibrosis is most important and effective, such as antivirals, quitting alcohol consumption, and weight loss[1]. However, effects of etiological treatment are limited and insufficient, and difficult to prevent the development of liver fibrosis into cirrhosis. At present, liver transplantation is a radical cure for cirrhosis but is associated with a high cost, organ shortages, and the risk of immune rejection[6]. In addition, almost all current clinical trials targeting fibrosis are focused on non-alcoholic steatohepatitis, specifically focusing on hepatic stellate cell (HSC) activation and/or fibrogenesis[7]. However, there are still no approved antifibrotic therapies for liver fibrosis[7]. Therefore, it is urgent to develop new effective drugs.

Developing new drugs is a difficult, high-cost, and extremely low success rate procedure[8]. A good strategy to address this problem is to investigate new indications of old drugs, a process called "drug repurposing"[9]. Scientists have repurposed many old drugs such as propranolol[10], cimetidine[11], sildenafil[12], and thalidomide[13]. Thus, drug repurposing is an attractive approach and has been widely employed. Drugs that have been approved by Food and Drug Administration (FDA) have passed preliminary clinical trials and are considered extremely safe. Therefore, FDA-approved drugs may be good candidates for developing new indications. Molecular docking, a fast, efficient, and widely

used technique in drug repurposing, is a computational strategy to predict binding sites between ligands and targets based on their structures[9,14].

The activation of HSCs is considered the central effector of liver fibrosis[15]. There are many associated signaling molecules, including transforming growth factor β (TGFβ), platelet-derived growth factor, and connective tissue growth factor[16]. The TGFβ signaling pathway plays a crucial role in the development of liver fibrosis[17]. A review paper illustrated that TGFβ1 activates TGFβ type II receptor (TGFβR2), followed by the recruitment of TGFβR1. Afterward, TGFβR2 phosphorylates TGFβR1 thereby triggering down-stream signaling pathway to regulate the expression of collagens and extracellular matrix (ECM)[18]. Therefore, TGFβR2 is considered an important target for developing drugs against liver fibrosis. Consistently, our group and others demonstrated that both inhibiting the expression of TGFβR2 and exogenous extracellular domain of TGFβR2 supplement effectively alleviated liver fibrosis [19,20].

In the current study, FDA-approved drugs were screened for binding affinity with the TGFβR2 by virtual molecular docking. We used cellular and mouse models to investigate its potential anti-liver fibrosis effect. In addition, by using mutagenesis analysis we further demonstrated detailed molecular working mechanism.

MATERIALS AND METHODS

Molecular docking of FDA-approved drugs and TGFβR2

The structures of FDA-approved drugs were downloaded from the ZINC database (https://zinc12.docking.org/). Then, the files of each small molecular structures were generated using Open Babel GUI (3.1.1). The TGFβR2-TGFβ1 complex (PDB: 3KFD) was downloaded from the Protein Data Bank (https://www.rcsb.org/). The TGFβR2 structure was derived from the TGFβR2-TGFβ1 complex using AutoDock Vina software (https://vina.scripps.edu/). AutoDock Vina software was employed to screen for the lowest energy complex among complexes of the extracellular TGFβR2 domain and the FDA-approved drugs.

Cell culture and viability experiments

The human HSC line LX-2 was purchased from the BeNa Culture Collection (Beijing, China) and cultured in Dulbecco's modified Eagle medium (DMEM, Gibco, United States) with 10% fetal bovine serum (FBS, Gibco, United States) at 37 °C in a 5% CO_2 atmosphere. LX-2 was activated by human recombinant protein TGFβ1 (5 ng/mL) for 24 h, followed by drug treatment for 24 h. The expression of fibrosis-related genes was analyzed.

Cell Counting Kit-8 (CCK-8, Beyotime Biotechnology, Shanghai, China) test was used to test the cytotoxicity of a series of working concentrations of the candidate drugs on LX-2 cell. After 24 h of treatment, the CCK-8 solution was added to each well for an additional 1 h of incubation (37 °C in a 5% CO_2 atmosphere). A microplate analyzer was used to measure the optical density of each well at 450 nm. Cell vitality was expressed as a percentage of optical density between the treatment wells and the negative control cells.

Determination of Kd value between TGFβR2 and dihydroergotamine

The Kd value of the small molecules and the TGFβR2 protein was measured using a microscale thermophoresis (MST)-Nanotemper instrument (Nanotemper, Germany). Micro thermophoresis is the directional movement of particles in the micro temperature gradient. The affinity is determined by measuring the change of micro thermophoresis caused by the change of hydration layer (usually caused by the change of biomolecular structure/conformation). First, 100 μL each of 10 μM TGFβR2 and different concentrations of the small molecules (diluted from 400 μM stock) were prepared. Second, TGFβR2 was labeled with a fluorescent dye and mixed with the small molecules. Third, fluorescence was measured to assess the binding behavior of the small molecule-TGFβR2 complex.

Molecular dynamics simulation

Molecular dynamics simulations were performed using Gromacs 2020.1, in which a charm36-mar2019 force field was chosen. The TGFβR2 or TGFβR2-small molecule complex was solved with TIP3P water and immersed in a dodecahedron box extending to at least 1 nm of the solvent on all sides. The system was neutralized with Na^+ and Cl^- by adding 0.15 M NaCl. It was energy-minimized using the steepest descent algorithm for 5000 steps and creating a maximum force of < 1000 kJ/mol/nm. After energy minimization, the system was equilibrated with a constrained "number of particles, volume, and temperature" (NVT) and "number of particles, pressure, and temperature" (NPT) running for 100 ps. Through NVT and NPT equilibration, the system was well-equilibrated at 300 K and 1 bar. Finally, MD simulations of the TGFβR2 or complex were carried out for 200 ns; trajectories were saved every 10 ps for analysis. The Verlet cut-off scheme and a Leap-frog integrator with a step size of 2 fs were applied. The modified Berendsen thermostat was used for temperature coupling, the Parrinello-Rahman barostat was used for pressure coupling, and the Particle Mesh Ewald method was used to determine long-range

electrostatic interactions.

The root-mean-square displacement (RMSD) and root-mean-square fluctuation (RMSF) of TGFβR2 and the complex were calculated using GROMACS 2020.1. The content of the secondary structure was calculated using DSSP software. The last MD simulation frame of the complex was extracted using GROMACS 2020.1. LigPlot+ software (https://www.ebi.ac.uk/thornton-srv/software/LigPlus/) was used to analyze the detailed interactions between the extracellular TGFβR2 domain and small molecule. PyMOL (http://www.pymol.org/) was used to prepare the structural images.

Production and purification of site-directed mutagenesis of TGFβR2

The binding sites of TGFβR2 and small molecule were established using the molecular docking results. The amino acids at the binding sites were mutated to alanine whose nucleotide sequence was GCG. The sequences of mutated extracellular TGFβR2 and a 6X His-tag were inserted into a pMAL-c5x plasmid that was synthesized by GenScript Biotech Corporation.

The mutated plasmid was transformed into BL21 (DE3) bacteria and induced with 0.8 mmol/L IPTG for 16 h at 28 °C. Then, bacteria were collected and resuspended in phosphate buffered saline (PBS). The mutated TGFβR2 protein was purified by HisTrap FF affinity chromatography and eluted with PBS containing gradient concentrations of imidazole. Finally, the eluted proteins were concentrated and the imidazole was removed by dialysis.

CCl_4 injury mouse model

Six-week-old male C57BL/6N mice were purchased from Vital River Laboratory Animal Technology Co. Ltd. to induce a liver fibrosis model. The animal protocol was designed to minimize pain or discomfort to the animals. The animals were acclimatized to laboratory conditions (23 °C, 12 h/12 h light/dark, 50% humidity, ad libitum access to food and water) for 2 wk prior to experimentation. After being transferred to our institute, the animals were randomly and evenly divided into four groups (eight mice per group) according to their body weight: Corn oil, carbon tetrachloride (CCl_4), low-concentration treatment, and high-concentration treatment groups. The same volume of CCl_4 (0.5 μL/g of body weight, Sigma-Aldrich, St. Louis, MO, United States) and corn oil were intraperitoneally injected three times a week to induce a liver fibrosis model and in control animals for four weeks, respectively. Intragastric gavage administration was carried out with conscious animals, using straight gavage needles appropriate for the animal size. Then, the small molecule aqueous solution and water was administered orally once a day as treatment and control for eight weeks, respectively. All animals were euthanized for tissue collection. All animal studies were performed following the National Institutes of Health's Guide for the Care and Use of Laboratory Animals and conducted with the approval of the Institutional Animal Care and Use Committee of the Institute of Zoology, Chinese Academy of Sciences.

B-mode ultrasonography

Small-animal B-ultrasound was used to inspect the portal veins. A high-resolution ultrasound imaging system (Vevo LAZR, VisualSonics, Canada) was used to measure the width and velocity of the portal vein. Mice were fasted for 12 h and shaved before the ultrasonic examination. Then, the mice were fixed on the platform and examined after being anesthetized with Avertin. After coating the mouse's abdomen with the coupling gel, the probe was used to inspect the mouse's portal vein.

Masson's trichrome staining

Mouse liver tissues were fixed in 4% paraformaldehyde, embedded in paraffin, and sectioned at 5 μm thickness. Then, the liver paraffin-embedded tissue sections were stained with a Masson's trichrome kit (G1281, Solarbio, Beijing, China) and observed under a 10x objective lens. Masson's trichrome staining is used to distinguish collagen fibrosis from muscle fibers. Muscle fibers were stained red and collagen fibrosis was stained green or blue. The collagen area was quantified using ImageJ 1.52a software. And one liver section was taken from each mouse for analysis.

Western blot analysis

Total proteins were extracted from the LX-2 cells or liver tissues using radioimmunoprecipitation assay lysis buffer (50 mmol/L Tris-HCl, pH 7.4; 1% NP-40; 0.25% sodium deoxycholate; 150 mmol/L NaCl; and 1 mmol/L ethylene diamine tetraacetic acid (EDTA)) containing a protease and phosphatase inhibitor mixture (Roche Diagnostics). The proteins were separated on 10% sodium dodecyl sulfate (SDS) polyacrylamide gels and transferred onto polyvinylidene fluoride membranes (Millipore). After blocking with 5% skim milk in Tris-buffered saline-Tween 20 (0.02 M Tris base, 0.1% Tween 20, 0.14 M NaCl, pH 7.4) for 1 h, the membranes were incubated with primary antibodies overnight at 4 °C. The membranes were then incubated with horseradish-peroxidase (HRP)-conjugated secondary antibodies for 1 h at room temperature. Supplementary Table 1 lists the antibodies.

Real-time quantitative PCR (RT-PCR) analysis

Total RNA was extracted from the LX-2 cells or liver tissues using TRIzolTM Reagent (Thermo Fisher Scientific, United States) according to the manufacturer's instructions. Complementary DNA (cDNA)

was obtained from the reverse-transcribed RNA using a high-capacity cDNA reverse-transcription kit (Promega, United States). The relative expression of genes was analyzed by RT-PCR (Light Cycler 480, Roche, Sweden) with SYBR Green Master Mix (Promega, United States). Supplementary Table 2 lists the primer sequences.

Isolation of liver mononuclear cells and flow cytometry analysis

Liver mononuclear cells (MNCs), including Kupffer cells, were isolated from mouse liver tissues. Liver samples were collected from mice under deep anesthesia. The liver samples were cut into pieces, transferred into 5 mL of enzyme mix [RPMI 1640 containing 1 mg/mL collagen IV (Sigma) and 20 U/mL DNase I (Roche, Burgess Hill, United Kingdom)], and digested in a water bath at 37 °C for 30 min. RPMI 1640 containing 10% FBS was added to arrest the digestion. The digested mixture was filtered through a 70 μm strainer, centrifuged at 4 °C for 10 min at 1000 × g, and the pellet was washed in PBS twice. Liver immune cells were subsequently isolated using a 33% Percoll cell separation solution after centrifuging for 25 min at 2200 × g at room temperature. The red blood cells were removed using a red blood cell lysis buffer (YESEN, Shanghai, China). Finally, liver immune cells were counted and stained with anti-F4/80 antibody eFluor® 450 (eBioscience, San Diego, CA), brilliant violet 510™-conjugated anti-CD45 antibody (Biolegend, San Diego, CA), and percp-cyanine5.5-conjugated anti-CD11b antibody (eBioscience, San Diego, CA), which were then filtered into flow tubes through a 0.45 μm strainer. The result of flow cytometry was analyzed using a BD Fortessa instrument (BD, NY, United States).

Plasma biochemical markers

Mouse blood samples were collected from the tail vein, collected into EDTA-containing tubes, and gently shaken. Plasma was collected after centrifuging at 3000 × g for 15 min at 4 °C. Plasma alanine aminotransferase (ALT) and aspartate aminotransferase (AST) levels were measured using a biochemistry analyzer (Cobas c 501, Roche, Sweden).

Statistical analyses

Data are expressed as mean ± standard error of the mean. The statistical significance between groups was analyzed using one-way ANOVA test. Statistical significance was set at $P < 0.05$ and $P < 0.05$, $P < 0.01$, $P < 0.001$, and $P < 0.0001$ were denoted as a, b, c, and d, respectively. GraphPad Prism software was used to perform all statistical analyses.

RESULTS

The docking analysis of FDA-approved small molecule drugs and TGFβR2

AutoDock Vina software was employed to dock drugs with the extracellular domain of TGFβR2 and output the complex structures. The complex and the binding sites of TGFβR2 and TGFβ1 were shown (Figure 1A), and the structure of TGFβR2 was split from the complex (Figure 1B). The binding affinity of each FDA-approved drug was evaluated (Figure 1C). Among those, darifenacin, cyproheptadine, lifitegrast, difenoxin, phenytoin, dihydroergotamine (DHE), naldemedine, and irinotecan showed higher scores out of 1615 drugs (Figure 1C). Darifenacin is a competitive muscarinic M receptor antagonist used to treat urinary frequency, urgency, and incontinence caused by bladder hyperstimulation[21]. Cyproheptadine is an antihistamine used to treat allergies[22]. Lifitegrast is a small molecule integrin inhibitor primarily used to treat symptoms and signs of dry eye[23]. Difenoxin is a human metabolite of diphenoxylate, which is a derivative of pethidine and can be used to treat functional diarrhea and chronic enteritis[24]. Phenytoin is an effective voltage-gated Na^+ channel blocker used to treat epilepsy, neuralgia, and arrhythmia[25]. DHE is an adrenergic receptor antagonist used to treat severe orthostatic hypotension, migraine, and headache[26], which can bind with various receptors. DHE is also an agonist at 5-HT1B, 5-HT1D, and 5-HT1F receptors, but it also binds to 5-HT1A and 5-HT2A receptors. Naldemedine is an opioid receptor antagonist used to treat non-cancerous pain and opioid-induced constipation[27]. Irinotecan is a semi-synthesis of water-soluble camptothecin derivatives used to treat advanced colorectal cancer and postoperative adjuvant chemotherapy[28] (Table 1). All the above drugs were purchased from Selleck Chemicals, except for difenoxin and naldemedine which are banned from purchase as they are under management control. Therefore, we performed the following experiments using the rest 6 small molecule drugs.

Cytotoxicity of candidate drugs

To investigate the cytotoxicity of these drugs, LX-2 cells were treated with 20 μM of each candidate for 24 h. The results demonstrated that irinotecan and cyproheptadine were cytotoxic to LX-2 cells at this concentration (Figure 1D). Therefore, irinotecan and cyproheptadine were regarded as cytotoxic drugs and excluded from subsequent experiments. Next, to identify the best range of concentrations that would not influence the viability of these cells, LX-2 cells were treated with different concentrations of the remaining drugs for 24 h. The results demonstrated that neither lifitegrast nor phenytoin was

Table 1 The drugs with the highest affinity of transforming growth factor β type II receptor

Name	ZINC_ID	Affinity (kcal/mol)	Indications
Darifenacin	ZINC000001996117	-7.6	Urinary frequency, urgency, and incontinence caused by bladder hyperstimulation
Cyproheptadine	ZINC000000968264	-7.4	Allergy
Lifitegrast	ZINC000084668739	-7.4	Symptoms and signs of dry eye
Difenoxin	ZINC000000601317	-7.3	Functional diarrhea and chronic enteritis
Phenytoin	ZINC000002510358	-7.3	Epilepsy, neuralgia, and arrhythmia
DHE	ZINC000003978005	-7.3	Severe orthostatic hypotension, migraine, and headache
Naldemedine	ZINC000100378061	-7.3	Non-cancerous pain and opioid induced constipation
Irinotecan	ZINC000001612996	-7.3	Advanced colorectal cancer and postoperative adjuvant chemotherapy

DHE: Dihydroergotamine.

cytotoxic to LX-2 cells when concentrations were up to 100 μM and 150 μM, respectively (Figure 1E and F). Darifenacin and DHE were cytotoxic to LX-2 cells when concentrations were beyond 50 μM and 20 μM, respectively (Figure 1G and H). Therefore, to avoid interference on fibrosis-related gene expression due to the cytotoxicity of candidate drugs, lifitegrast and phenytoin concentrations below 100 μM and darifenacin and DHE concentrations below 20 μM were used to treat LX-2 cells.

Anti-fibrotic effect of candidate drugs in cellular model

Increased expression of collagen and alpha-smooth muscle actin (α-SMA) are principal markers of HSC activation[29]. LX-2 cells were treated with different concentrations of drugs for 24 h after TGFβ1 stimulation. The results demonstrated that lifitegrast and phenytoin did not decrease the protein levels of collagen III and α-SMA after TGFβ1 stimulation (Figure 2A and B). Moreover, darifenacin did not decrease the protein levels of collagen III, p-SMAD3, and α-SMA as much as DHE (Figure 2C and D). Consistently, DHE significantly decreased the mRNA expression of collagen I alpha 1 (COL1A1), collagen I alpha 2 (COL1A2), collagen III alpha 1 (COL3A1), and α-SMA compared with darifenacin (Figure 2E and F). Taken together, DHE (PubChem CID: 10531) was the most effective small molecule drug that suppressed the TGFβ1 induced LX-2 activation.

The binding affinity of DHE to TGFβR2

We further verified the molecular docking result by MST-Nanotemper. The results demonstrated that the fluorescence intensity of TGFβR2 changed gradually in proportion to the DHE concentration (Figure 3A). The affinity is determined by measuring the change of micro thermophoresis caused by the change of hydration layer, and results showed the binding affinity of DHE to TGFβR2 with a Kd value of 17.64 μM.

Molecular dynamics simulation of DHE and TGFβR2

To identify the specific binding mode of DHE and TGFβR2, we used the complex structure obtained from AutoDock vina to perform the molecular dynamics simulation with GROMACS 2020.1 software for 200 ns. The results demonstrated that the RMSD of the backbone atoms of TGFβR2 and TGFβ R2□DHE in the simulation system reached equilibrium after 100 ns (Figure 3B). The RMSFs of the TGFβ R2 skeleton carbon atoms in the two simulated systems were almost identical (Figure 3C). The secondary structural elements of TGFβR2 in the complex simulation were only slightly changed (Figure 3D and Table 2). The coil and 3-helix components of TGFβR2 decreased in the complex simulation system (Table 2). Finally, we extracted the simulated complex structure and analyzed the amino acid sites of TGFβR2 bound to DHE by Ligplot+ software (Figure 3E and F). In conclusion, our molecular dynamics simulations showed that the binding of DHE to TGFβR2 has little effect on the structure of TGFβR2. We also obtained the binding sites of TGFβR2 to DHE by stimulations.

Leu27, Phe30, Thr51, Ser52, Ile53, and Glu55 of TGFβR2 bind with DHE

Molecule docking demonstrated that Leu27, Phe30, Thr51, Ser52, Ile53, and Glu55 of TGFβR2 were binding sites for DHE (Figure 3F). To verify these binding sites, we mutated the above-mentioned amino acids to alanine. The DNA sequences of mutated extracellular TGFβR2 were synthesized (Table 3) and the binding affinity was measured. The results demonstrated that the mutated TGFβR2 no longer bound to DHE (Figure 3G). Thus, the above-mentioned binding sites of TGFβR2 predicted by molecule docking were the exact binding sites of TGFβR2 and DHE, and this further verified the binding of TGFβR2 and DHE. Therefore, we inferred that the binding of TGFβ1 and TGFβR2 was

Table 2 Content of secondary structural analysis from DSSP method

Structure	Coil	β-Sheet	β-Bridge	Bend	Turn	3-Helix
TGFβR2	0.58	0.3	0.42	0.02	0.12	0.13
TGFβR2-DHE	0.56	0.3	0.42	0.02	0.12	0.12

TGFβR2: Transforming growth factor β type II receptor; DHE: Dihydroergotamine.

Table 3 DNA sequence of extracellular transforming growth factor β type II receptor before and after mutation

	Before mutation	After mutation
DNA sequence of TGFβR2 extracellular domain	ACGATCCCACCGCACGTTCAGAAGTCGGTTAATAACGACA TGATAGTCACTGACAACAACGGTGCAGTCAAGTTTCCACA ACTGTGTAAATTTTGTGATGTGAGATTTTCCACCTGTGACA ACCAGAAATCCTGCATGAGCAACTGCAGCATCACCTCCA TCTGTGAGAAGCCACAGGAAGTCTGTGTGGCTGTATGGA GAAAGAATGACGAGAACATAACACTAGAGACAGTTTGCC ATGACCCCAAGCTCCCCTACCATGACTTTATTCTGGAAGAT GCTGCTTCTCCAAAGTGCATTATGAAGGAAAAAAAAAAGC CTGGTGAGACTTTCTTCATGTGTTCCTGTAGCTCTGATGAG TGCAATGACAACATCATCTTCTCAGAAGAATATAACACCA GCAATCCTGACTTGTTGCTAGTCATATTTCAA	ACGATCCCACCGCACGTTCAGAAGTCGGTTAATAACGACA TGATAGTCACTGACAACAACGGTGCAGTCAAGTTTCCACA AGCGTGTAAAGCGTGTGATGTGAGATTTTCCACCTGTGACA ACCAGAAATCCTGCATGAGCAACTGCAGCATCGCGGCGG CGTGTGCGAAGCCACAGGAAGTCTGTGTGGCTGTATGGA GAAAGAATGACGAGAACATAACACTAGAGACAGTTTGCC ATGACCCCAAGCTCCCCTACCATGACTTTATTCTGGAAGAT GCTGCTTCTCCAAAGTGCATTATGAAGGAAAAAAAAAAGC CTGGTGAGACTTTCTTCATGTGTTCCTGTAGCTCTGATGAG TGCAATGACAACATCATCTTCTCAGAAGAATATAACACCA GCAATCCTGACTTGTTGCTAGTCATATTTCAA

TGFβR2: Transforming growth factor β type II receptor.

blocked by the binding of DHE and TGFβR2, further preventing the TGFβ signaling cascade.

DHE alleviated liver fibrosis in mouse

To explore whether DHE could alleviate fibrosis in vivo, we used two different concentrations of DHE to treat a CCl_4-induced mouse fibrosis model. Six-week-old C57BL/6N mice were intraperitoneally injected three-time per week with CCl_4 and corn oil (control group) during the whole experimental periods (Supplementary Figure 1). After four weeks, the mice intraperitoneally injected with CCl_4 were randomly divided into three groups: CCl_4 and the 2 and 5 mg/kg DHE treatment groups. The aqueous solution of DHE was orally gavaged to the mice in the treatment groups. For vehicle treatment, water was provided by oral gavage to the mice in the corn oil and CCl_4 group (disease group).

It is well known that more serious the degree of liver fibrosis, the wider the portal vein and the slower its velocity. The results demonstrated that the portal vein in the CCl_4 group was significantly wider than that in the corn oil group. Interestingly, the width of the portal vein in the 2 mg/kg DHE treatment group was significantly decreased (Figure 4A). Furthermore, the velocity of the portal vein in the treatment groups was also improved (Figure 4B). After eight weeks of treatment, there were no significant differences in body weight, liver weight, spleen weight, or the ratio of liver weight to body weight among the four groups (Figure 4C and Supplementary Figure 2A). Gross liver specimens of the CCl_4 group were paler and had a rough appearance. However, it was back to normal appearance by DHE treatment compared to the CCl_4 group (Figure 4D). The level of plasma ALT of the CCl_4 group mice was significantly higher than corn oil group. Whereas, DHE treatment significantly decreased the level of ALT compared with CCl_4 group mice. In addition, the level of plasma AST was significantly decreased after 2 mg/kg DHE treatment (Figure 4E). Collagen area were visualized by Masson's trichrome and quantified by using ImageJ 1.52a software. DHE treatment in both dosages significantly reduced collagen accumulation compared with those of the CCl_4 group (Figure 4F and G). Taken together, these results demonstrated that DHE significantly protected from liver fibrosis in CCl_4-induced mouse fibrosis model.

DHE decreased the liver macrophages infiltration and ECM deposition

The infiltration of macrophages reflects the severity of liver inflammation. To investigate the degree of macrophages infiltration, the liver immune cells were extracted and labeled with $CD45^+$, $F4/80^+$, and $CD11b^+$ antibodies followed by flow-cytometric analysis. The results demonstrated that the DHE treatment at both dosages significantly reduced proportion of $CD11b^+$ cells (Figure 5A and B, and Supplementary Figure 2B-F). Consistent with the result of flow cytometry, the mRNA levels of tumor necrosis factor alpha (TNFα) and F4/80 which are two important indicators of liver inflammation significantly decreased upon DHE treatment (Figure 5C). On the other hand, the accumulation of ECM is another important sign of liver fibrosis. The results demonstrated that the mRNA levels of COL1A1, COL1A2, and α-SMA significantly decreased in the DHE treatment group more than those of the CCl_4 group (Figure 5D). The mRNA levels of COL3A1 also decreased in the DHE treatment groups

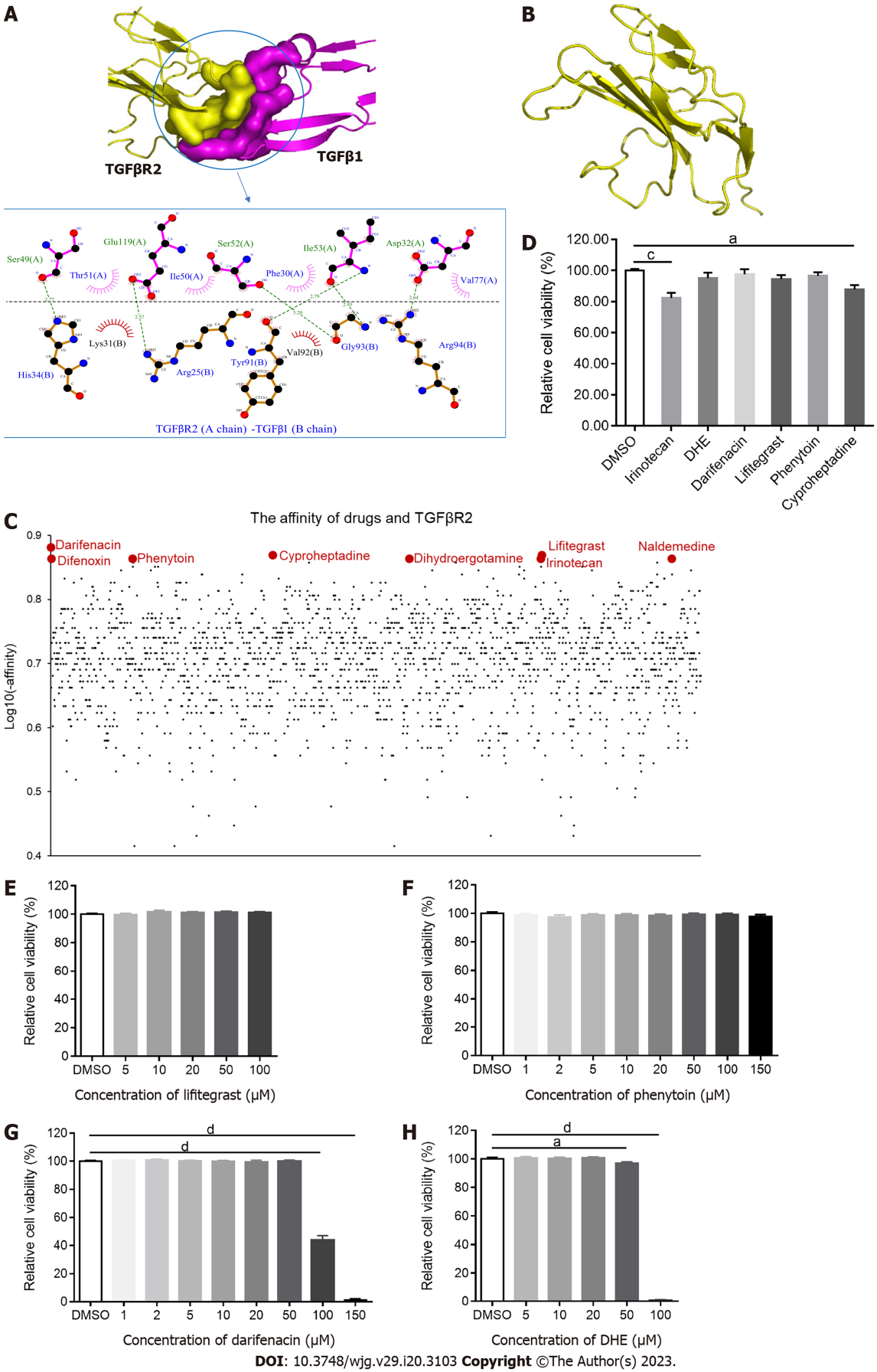

DOI: 10.3748/wjg.v29.i20.3103

Figure 1 Screening Food and Drug Administration-approved drugs for binding to transforming growth factor β type II receptor. A: The combination of transforming growth factor β type II receptor (TGFβR2) and transforming growth factor β 1 (TGFβ1); B: The structure of TGFβR2; C: The affinity of

each Food and Drug Administration-approved drug and TGFβR2. The affinity of TGFβR2 and darifenacin, cyproheptadine, lifitegrast, difenoxin, phenytoin, dihydroergotamine (DHE), naldemedine, and irinotecan was -7.6, -7.4, -7.4, -7.3, -7.3, -7.3, -7.3, and -7.3 kcal/mol, respectively; D: Cell viability of LX-2 treated with 20 μM of the drugs for 24 h (n = 5); E-H: Cell viability following LX-2 treatment with different concentrations of darifenacin, DHE, lifitegrast, and phenytoin for 24 h (n = 6). All data are presented as mean ± standard error of the mean. One-way ANOVA test was performed. [a]P < 0.05, [b]P < 0.01, [c]P < 0.001, and [d]P < 0.0001. TGFβ: Transforming growth factor β; TGFβR: Transforming growth factor β receptor; DHE: Dihydroergotamine.

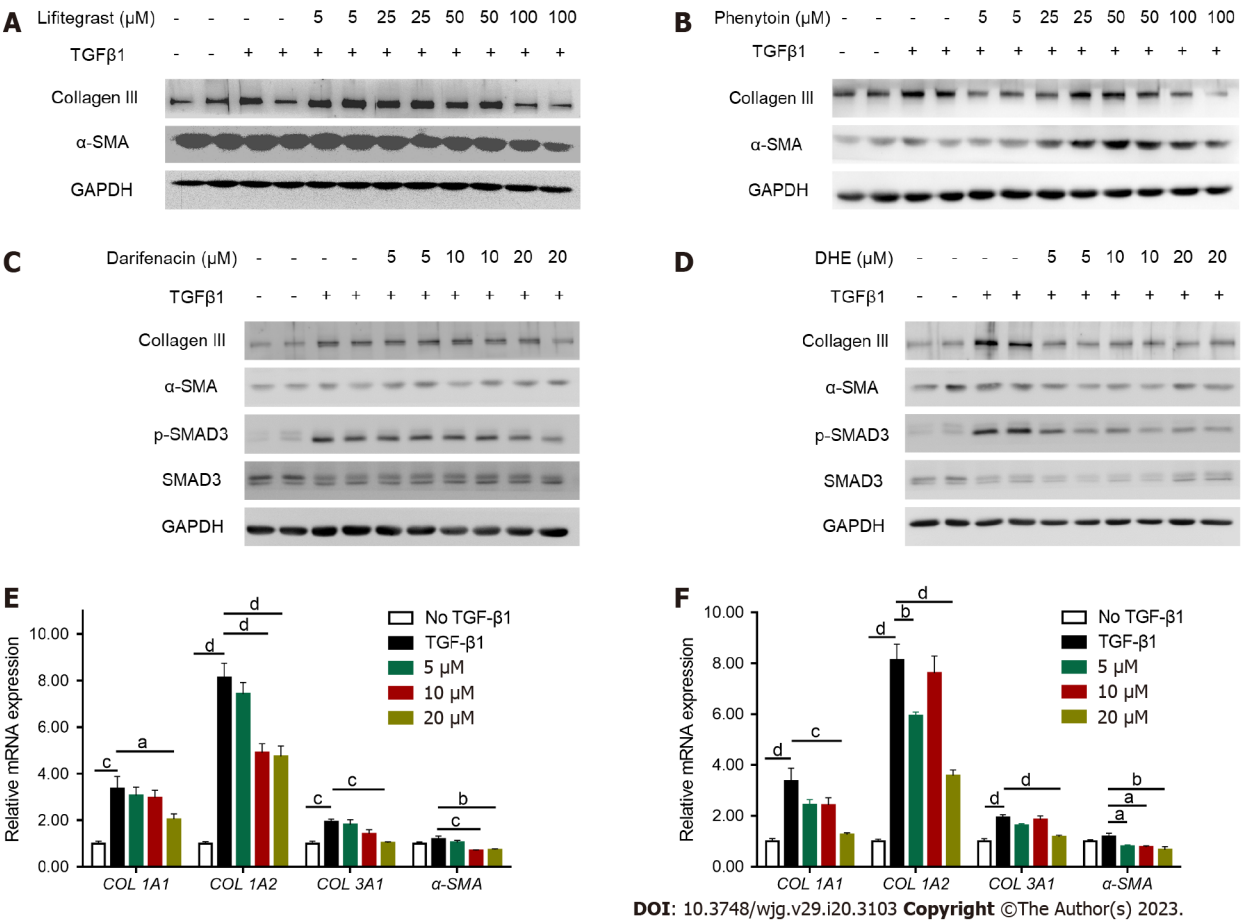

DOI: 10.3748/wjg.v29.i20.3103

Figure 2 Treatment inhibiting the activation of LX-2 cells. A and B: After LX-2 cell was activated with transforming growth factor β 1 (TGFβ1) (5 ng/mL) for 24 h, different concentrations of lifitegrast and phenytoin were added for 24 h, and the protein levels of collagen III and α-SMA were detected by western blot; C and D: After LX-2 was activated with TGFβ1 (5 ng/mL) for 24 h, different concentrations of darifenacin and dihydroergotamine (DHE) were added for further treatment for 24 h, and the protein levels of collagen III, α-SMA, and p-SMAD3 were detected by western blot; E: Real-time polymerase chain reaction (RT-PCR) was performed to detect the expression of COL1A1, COL1A2, COL3A1, and α-SMA of LX-2 after different concentrations of darifenacin treatment (n = 6); F: RT-PCR was performed to detect the expression of COL1A1, COL1A2, COL3A1, and α-SMA of LX-2 after different concentrations of DHE treatment (n = 5-6). All data are presented as means ± standard error of the mean. One-way ANOVA test was performed. [a]P < 0.05, [b]P < 0.01, [c]P < 0.001, and [d]P < 0.0001. TGFβ: Transforming growth factor β; TGFβR: Transforming growth factor β receptor; DHE: Dihydroergotamine.

(Figure 5D). Meanwhile, the protein levels of α-SMA and p-SMAD3 were significantly decreased in the DHE treatment group compared to those of the CCl_4 group (Figure 5E and F). Thus, we demonstrated here that, DHE significantly decreased the liver macrophages infiltration and ECM deposition.

DISCUSSION

TGFβ1 is regarded as the most potent fibrogenic cytokine, which activates TGFβR2, followed by the recruitment of TGFβR1, therefore triggers HSC activation[30]. In the current study, we aimed to screen drugs targeting TGFβR2 and further blocking TGFβ down-stream signaling pathway from FDA-approved small molecule library. Among these 6 candidate drugs, DHE significantly decreased the protein and mRNA expression of fibrotic-related genes in LX-2 cells. The results of the affinity experiment demonstrated that DHE binds with TGFβR2 at Leu27, Phe30, Thr51, Ser52, Ile53, and Glu55. DHE also significantly alleviated liver fibrosis by decreasing macrophages infiltration and ECM accumulation in CCl_4-induced mouse fibrosis model. Thus, we demonstrate here for the first time that

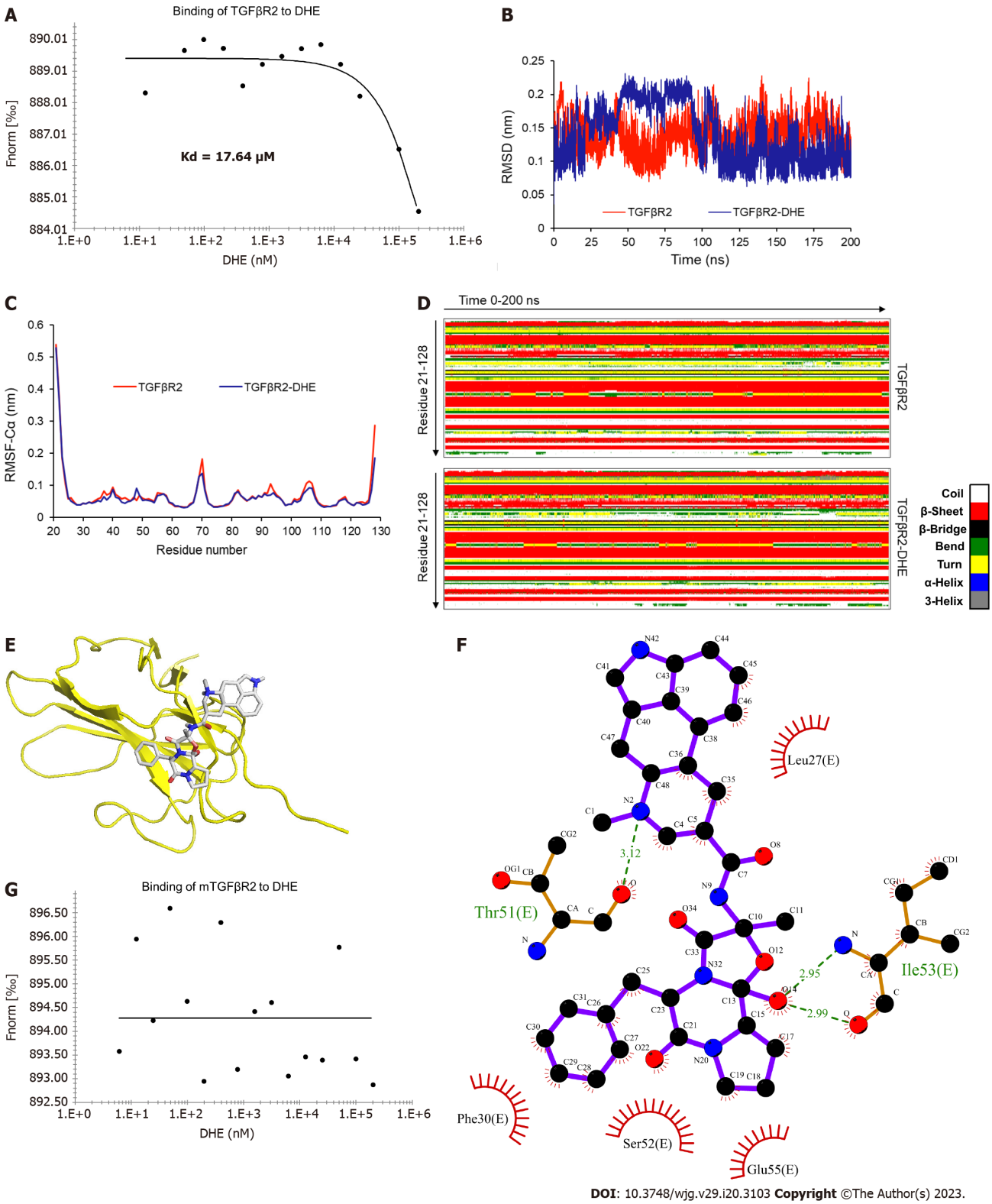

DOI: 10.3748/wjg.v29.i20.3103 **Copyright** ©The Author(s) 2023.

Figure 3 The binding affinity and sites of dihydroergotamine and transforming growth factor β type II receptor. A: Transforming growth factor β type II receptor (TGFβR2) bound to dihydroergotamine (DHE) with a Kd of 17.64 μM; B: Molecular dynamics simulation results of DHE and TGFβR2. Root-mean-square deviation of TGFβR2 skeleton atom; C: Root-mean-square fluctuation of backbone Cα atoms of TGFβR2 skeleton atom; D: The secondary structure components of TGFβR2 and complex simulation systems in 0-200 ns; E and F: The binding sites of DHE and TGFβR2; G: The binding affinity of TGFβR2 mutants with DHE. TGFβ: Transforming growth factor β; TGFβR: Transforming growth factor β receptor; DHE: Dihydroergotamine.

DHE, an anti-headache agent, is used in the treatment of liver fibrosis.

Developing a new drug needs more than a decade and significant investment[8]. Drug repurposing is a potential tool to accelerate the drug discovery process, which has been employed to develop therapies for coronavirus disease 2019[31], antimicrobials[32], and rare diseases[33]. The chemical structure of DHE is similar to that of many natural neurotransmitters, including epinephrine, norepinephrine,

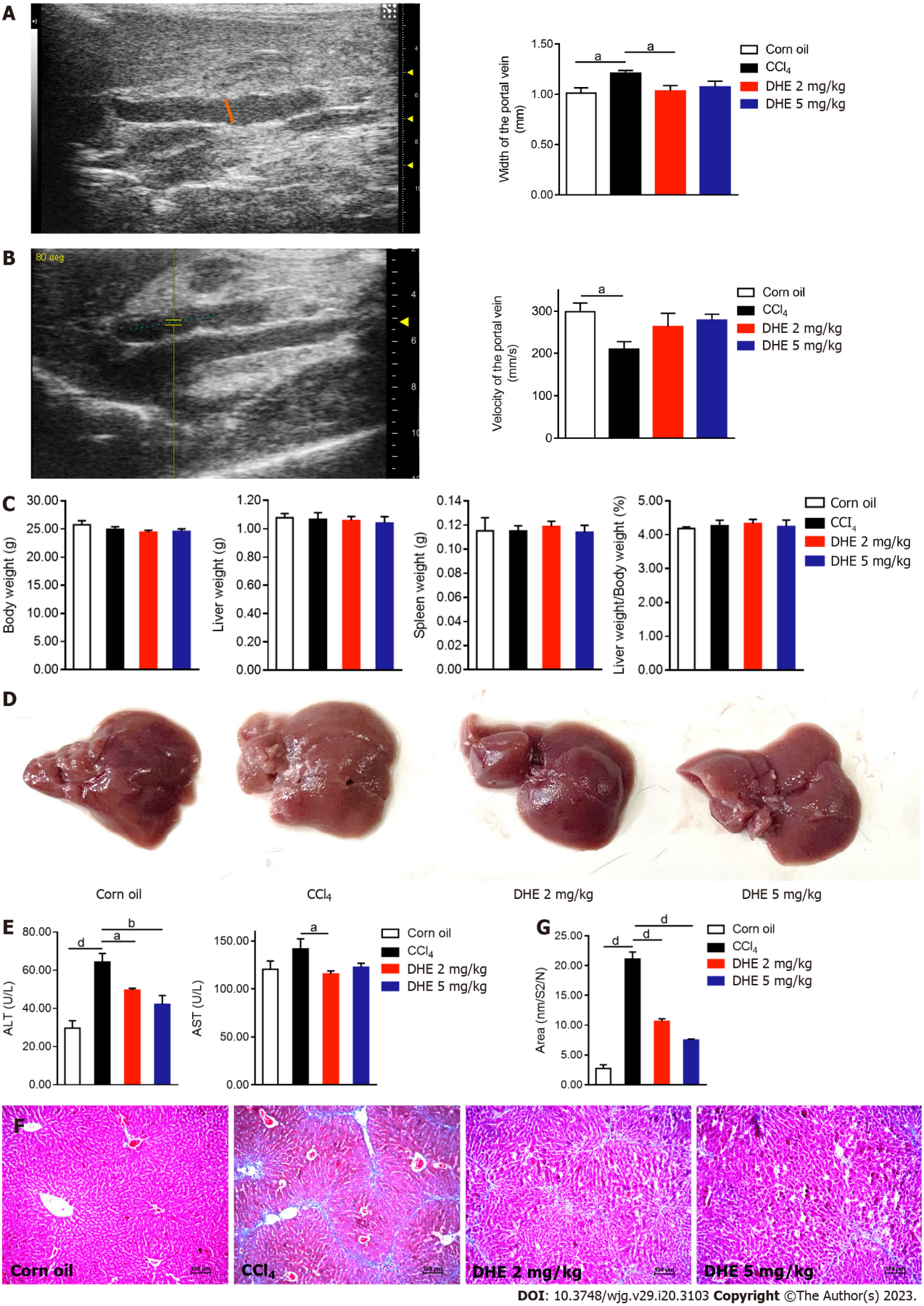

DOI: 10.3748/wjg.v29.i20.3103 **Copyright** ©The Author(s) 2023.

Figure 4 Dihydroergotamine alleviated fibrosis in CCl_4-induced liver fibrosis model mice. A: The width of the portal vein (left panel); portal vein width of mice in each group (right panel, *n* = 7); B: The velocity of the portal vein (left panel); the velocity of mice in each group (right panel, *n* = 7); C: Body weight,

liver weight, spleen weight, and liver weight/body weight of mice in each group (n = 6-8); D: Gross liver specimens of the mice in each group; E: An automated biochemistry analyzer determined the enzymatic activities of serum levels of alanine aminotransferase and aspartate aminotransferase (n = 6-7); F: Masson's trichrome staining was performed on liver sections; G: Collagen area in Masson's trichrome staining (n = 7-8). All data were presented as means ± standard error of the mean. One-way ANOVA test was performed. $^{a}P < 0.05$, $^{b}P < 0.01$, $^{c}P < 0.001$, and $^{d}P < 0.0001$. TGFβ: Transforming growth factor β; TGFβR: Transforming growth factor β receptor; DHE: Dihydroergotamine.

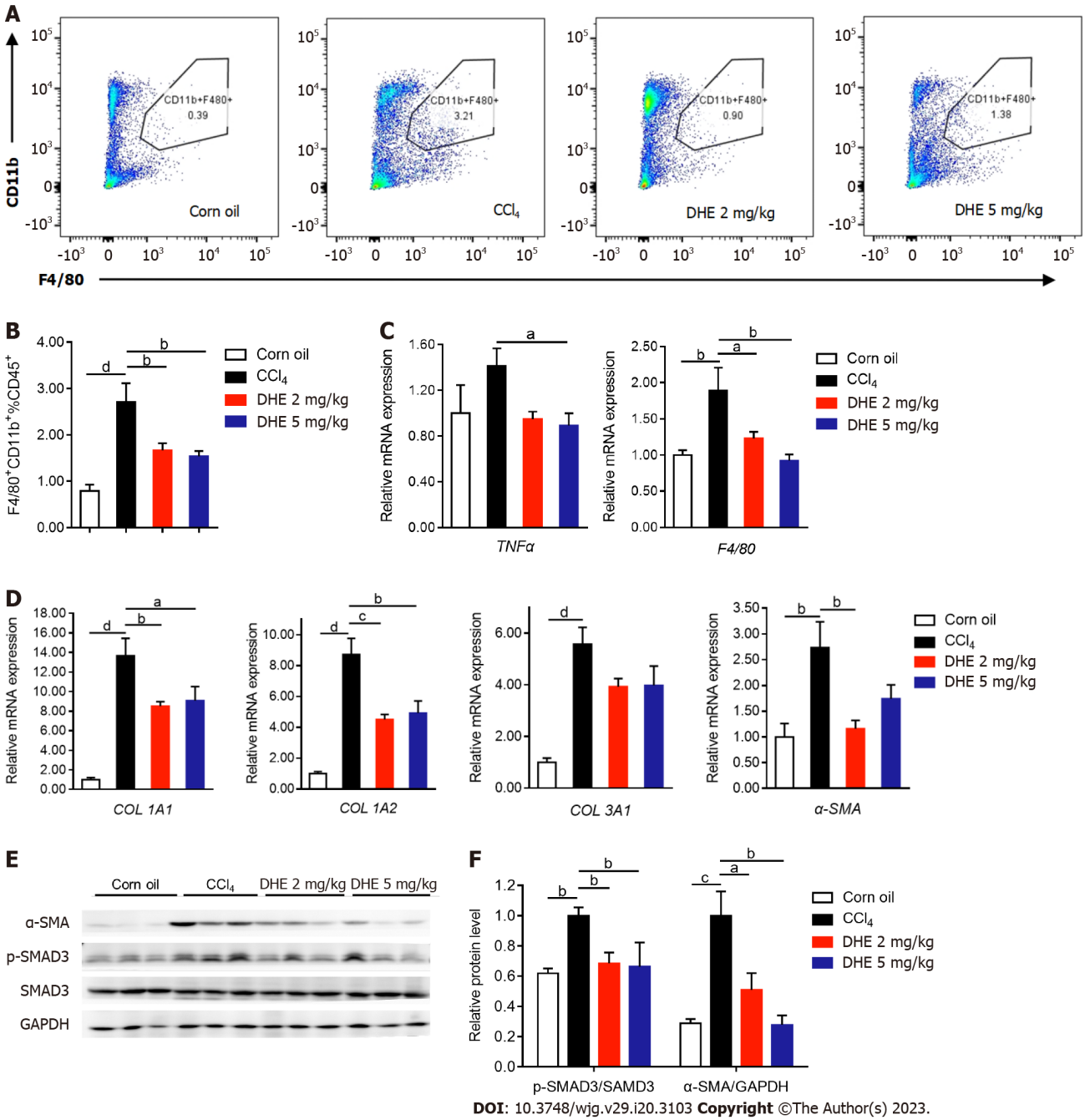

DOI: 10.3748/wjg.v29.i20.3103 **Copyright** ©The Author(s) 2023.

Figure 5 Dihydroergotamine decreased the inflammatory infiltration of macrophages and extracellular matrix deposition in the liver. A and B: The flow cytometric analysis of CD11b^{+} cells (n = 6-8); C: The effects of dihydroergotamine (DHE) treatment on the mRNA expression levels of inflammation-related genes (n = 6-8); D: The effects of DHE treatment on the mRNA expression levels of extracellular matrix-related genes (n = 6-8); E: The protein levels of p-SMAD3 and α-SMA in liver tissues of mice in each group were detected by western blot (n = 3). All data are presented as means ± standard error of the mean. One-way ANOVA test was performed. $^{a}P < 0.05$, $^{b}P < 0.01$, $^{c}P < 0.001$, and $^{d}P < 0.0001$. TGFβ: Transforming growth factor β; TGFβR: Transforming growth factor β receptor; DHE: Dihydroergotamine.

dopamine, and serotonin[26]. It can modulate noradrenergic, serotonergic, and dopaminergic neurotransmission[34]. DHE is an adrenergic receptor antagonist used to treat severe orthostatic hypotension, migraine, and headache[26], which can bind with various receptors. DHE is also an

agonist of 5-HT1B, 5-HT1D, and 5-HT1F receptors, but it also binds to 5-HT1A and 5-HT2A receptors [26]. In the current study, surprisingly, we found that DHE also bind with TGFβR2 at reasonable affinity. Furthermore, we also identified specific binding sites by mutagenesis analysis. These results imply that DHE not only specifically targets 5-HT, but also TGFβR2. It further highlights wide-spread function of DHE in physiology/pathophysiology.

Continuous local and systemic inflammation aggravates liver injury, which is a critical factor in liver fibrosis. The innate immune system plays a pivotal role from the onset to the end stage of chronic liver disease[35]. Hepatic macrophages are considered as the first line of defense against pathogens, are a key cellular determinant in the process of fibrosis[36]. Bone marrow monocyte-derived macrophages and Kupffer cells are two distinct subsets of macrophages in the liver, which have been identified as key regulators of liver inflammation and key to the progression or regression of liver fibrosis. Kupffer cells, which are resident macrophages in liver tissue, exert anti-inflammatory effects[37]. Activated macrophages produce large amounts of TGFβ, which activates HSC into myofibroblast-like cells and synthesizes ECM[38]. This inflammatory response is also evident in the CCl_4-induced mouse model, especially in the increased number of macrophages in liver. Consistent with previous results, we also found that the macrophages infiltration was significantly increased after CCl_4 treatment. We speculate that, upon binding to TGFβR2, DHE prevents recruitment of TGFβR1 to TGFβR2, thereby inhibiting TGF β down-stream signaling pathway. Consistently, F4/80 and TNFα mRNA expression also significantly decreased upon DHE treatment. Taken together, DHE might reduce macrophages infiltration and finally prevent liver inflammation.

Activated HSCs secreting ECM represent a critical event in development of liver fibrosis[37]. In the fibrotic liver, type I and III collagens are deposited instead of laminins, type IV collagen, and proteoglycans in the normal liver[17]. Various mechanisms of HSC activation have been postulated, including TGFβ/SMAD pathway, Notch, Wnt/β-catenin, Hedgehog, and Hippo signaling[16]. In the current study, we revealed that DHE significantly reduced TGFβ induced HSCs activation in LX-2 cellular model through specific blocking of TGFβ signaling pathway. It explained clearly the significant reduction of ECM by DHE treatment. Taken together, our data show that DHE alleviated liver fibrosis by binding to TGFβR2, preventing the binding of TGFβ1 and TGFβR2, and blocking TGFβ1 signaling to reduce liver inflammation.

CONCLUSION

Our study demonstrated that DHE alleviated liver fibrosis while decreasing inflammation-related gene expression and HSC activation. The mechanism of its action is likely to be associated with decreased macrophages infiltration and ECM accumulation. Considering that liver fibrosis can be reversed, DHE might open-up new avenue to treat liver fibrosis in the future.

ARTICLE HIGHLIGHTS

Research background

The transforming growth factor β (TGFβ) signaling pathway plays a crucial role in the development of liver fibrosis by activating TGFβ type II receptor (TGFβR2), followed by the recruitment of TGFβR1 finally triggering downstream signaling pathway.

Research motivation

TGFβR2 is considered an important target for developing drugs against liver fibrosis. Previous studies demonstrated that both inhibiting the expression of TGFβR2 and exogenous extracellular domain of TGFβR2 supplement effectively alleviated liver fibrosis.

Research objectives

To find drugs targeting TGFβR2 that inhibit TGFβR1/TGFβR2 complex formation, theoretically inhibit its downstream TGFβ signaling pathway, and thereby ameliorate liver fibrosis, we screened drugs approved by the Food and Drug Administration (FDA) to identify potential TGFβR2 blockers.

Research methods

FDA-approved drugs were screened for binding affinity with TGFβR2 by virtual molecular docking. We identified 6 candidates and further explored their potential by Cell Counting Kit-8 cell cytotoxic experiment to validate toxicity and titrated the best cellular working concentrations. Next, we further demonstrated the detailed molecular working mechanisms using mutagenesis analysis. Finally, we used a mouse model to investigate its potential anti-liver fibrosis effect.

Research results

Dihydroergotamine (DHE) shows great ability in reducing fibrotic gene expressions such as collagen, p-SMAD3, and α-SMA in TGFβ induced cellular model of liver fibrosis in LX-2 cells. Furthermore, we demonstrated that DHE binds to TGFβR2 with a Kd value of 17.64 μM. In addition, DHE significantly improved liver fibrosis, as evidenced by Masson's trichrome staining of liver sections, the width and the velocity of the portal vein, and serum markers of liver function. In line with those observations, DHE also decreased macrophages infiltration and extracellular matrix deposition in the liver.

Research conclusions

DHE could alleviate liver fibrosis by binding to TGFβR2 thereby suppressing its downstream TGFβ signaling pathway. We show here that as far as drug repurposing, DHE has great potential to treat liver fibrosis.

Research perspectives

Considering that liver fibrosis can be reversed, DHE might open-up new avenue to treat liver fibrosis in the future.

FOOTNOTES

Author contributions: Xie W designed experiments and revised the manuscript; Jin WZ and Wang Q reversed the manuscript; Zheng KX and Yuan SL performed experiments, analyzed data, and wrote the manuscript; Dong M and Zhang HL performed experiments, analyzed data, and revised the manuscript; Other authors helped with the experiments; All authors read and approved the final version of the article.

Supported by the Special Research Project for Capital Health Development, No. 2022-2-2174; and the Beijing Municipal Science and Technology Commission, No. Z191100007619037.

Institutional animal care and use committee statement: All procedures involving animals were reviewed and approved by the Institutional Animal Care and Use Committee the Institute of Zoology, Chinese Academy of Sciences, IACUC protocol No. IOZ-IACUC-2020-114.

Conflict-of-interest statement: Dr. Xie reports in addition, Dr. Xie has a patent Application of dihydroergotamine in the treatment of liver fibrosis issued.

Data sharing statement: No additional data are available.

ARRIVE guidelines statement: The authors have read the ARRIVE guidelines, and the manuscript was prepared and revised according to the ARRIVE guidelines.

Country/Territory of origin: China

ORCID number: Ke-Xin Zheng 0000-0002-8252-1170; Shou-Li Yuan 0000-0002-4733-9891; Zhi Zhang 0000-0002-2471-1494; Qi Wang 0000-0002-0269-1568; Wen Xie 0000-0002-7314-8175.

S-Editor: Li L
L-Editor: A
P-Editor: Yuan YY

REFERENCES

1 **Parola M**, Pinzani M. Liver fibrosis: Pathophysiology, pathogenetic targets and clinical issues. *Mol Aspects Med* 2019; **65**: 37-55 [PMID: 30213667 DOI: 10.1016/j.mam.2018.09.002]

2 **Pellicoro A**, Ramachandran P, Iredale JP, Fallowfield JA. Liver fibrosis and repair: immune regulation of wound healing in a solid organ. *Nat Rev Immunol* 2014; **14**: 181-194 [PMID: 24566915 DOI: 10.1038/nri3623]

3 **Karsdal MA**, Nielsen SH, Leeming DJ, Langholm LL, Nielsen MJ, Manon-Jensen T, Siebuhr A, Gudmann NS, Rønnow S, Sand JM, Daniels SJ, Mortensen JH, Schuppan D. The good and the bad collagens of fibrosis - Their role in signaling and organ function. *Adv Drug Deliv Rev* 2017; **121**: 43-56 [PMID: 28736303 DOI: 10.1016/j.addr.2017.07.014]

4 **Ginès P**, Krag A, Abraldes JG, Solà E, Fabrellas N, Kamath PS. Liver cirrhosis. *Lancet* 2021; **398**: 1359-1376 [PMID: 34543610 DOI: 10.1016/S0140-6736(21)01374-X]

5 **Marcellin P**, Gane E, Buti M, Afdhal N, Sievert W, Jacobson IM, Washington MK, Germanidis G, Flaherty JF, Aguilar Schall R, Bornstein JD, Kitrinos KM, Subramanian GM, McHutchison JG, Heathcote EJ. Regression of cirrhosis during treatment with tenofovir disoproxil fumarate for chronic hepatitis B: a 5-year open-label follow-up study. *Lancet* 2013; **381**: 468-475 [PMID: 23234725 DOI: 10.1016/S0140-6736(12)61425-1]

6 **Sapisochin G**, Bruix J. Liver transplantation for hepatocellular carcinoma: outcomes and novel surgical approaches. *Nat Rev Gastroenterol Hepatol* 2017; **14**: 203-217 [PMID: 28053342 DOI: 10.1038/nrgastro.2016.193]

7 **Friedman SL**, Pinzani M. Hepatic fibrosis 2022: Unmet needs and a blueprint for the future. *Hepatology* 2022; **75**: 473-488 [PMID: 34923653 DOI: 10.1002/hep.32285]

8 **Parvathaneni V**, Kulkarni NS, Muth A, Gupta V. Drug repurposing: a promising tool to accelerate the drug discovery process. *Drug Discov Today* 2019; **24**: 2076-2085 [PMID: 31238113 DOI: 10.1016/j.drudis.2019.06.014]

9 **Pushpakom S**, Iorio F, Eyers PA, Escott KJ, Hopper S, Wells A, Doig A, Guilliams T, Latimer J, McNamee C, Norris A, Sanseau P, Cavalla D, Pirmohamed M. Drug repurposing: progress, challenges and recommendations. *Nat Rev Drug Discov* 2019; **18**: 41-58 [PMID: 30310233 DOI: 10.1038/nrd.2018.168]

10 **Knight JM**, Kerswill SA, Hari P, Cole SW, Logan BR, D'Souza A, Shah NN, Horowitz MM, Stolley MR, Sloan EK, Giles KE, Costanzo ES, Hamadani M, Chhabra S, Dhakal B, Rizzo JD. Repurposing existing medications as cancer therapy: design and feasibility of a randomized pilot investigating propranolol administration in patients receiving hematopoietic cell transplantation. *BMC Cancer* 2018; **18**: 593 [PMID: 29793446 DOI: 10.1186/s12885-018-4509-0]

11 **Ramos-Arancibia N**, Varas C, Rozas-Muñoz E. Severe and recalcitrant periungual warts in a child successfully treated with cimetidine. *Dermatol Ther* 2021; **34**: e15154 [PMID: 34623743 DOI: 10.1111/dth.15154]

12 **Galiè N**, Ghofrani HA, Torbicki A, Barst RJ, Rubin LJ, Badesch D, Fleming T, Parpia T, Burgess G, Branzi A, Grimminger F, Kurzyna M, Simonneau G; Sildenafil Use in Pulmonary Arterial Hypertension (SUPER) Study Group. Sildenafil citrate therapy for pulmonary arterial hypertension. *N Engl J Med* 2005; **353**: 2148-2157 [PMID: 16291984 DOI: 10.1056/NEJMoa050010]

13 **Franks ME**, Macpherson GR, Figg WD. Thalidomide. *Lancet* 2004; **363**: 1802-1811 [PMID: 15172781 DOI: 10.1016/S0140-6736(04)16308-3]

14 **Yang J**, Roy A, Zhang Y. Protein-ligand binding site recognition using complementary binding-specific substructure comparison and sequence profile alignment. *Bioinformatics* 2013; **29**: 2588-2595 [PMID: 23975762 DOI: 10.1093/bioinformatics/btt447]

15 **Higashi T**, Friedman SL, Hoshida Y. Hepatic stellate cells as key target in liver fibrosis. *Adv Drug Deliv Rev* 2017; **121**: 27-42 [PMID: 28506744 DOI: 10.1016/j.addr.2017.05.007]

16 **Yan Y**, Zeng J, Xing L, Li C. Extra- and Intra-Cellular Mechanisms of Hepatic Stellate Cell Activation. *Biomedicines* 2021; **9** [PMID: 34440218 DOI: 10.3390/biomedicines9081014]

17 **Tsuchida T**, Friedman SL. Mechanisms of hepatic stellate cell activation. *Nat Rev Gastroenterol Hepatol* 2017; **14**: 397-411 [PMID: 28487545 DOI: 10.1038/nrgastro.2017.38]

18 **Fabregat I**, Moreno-Càceres J, Sánchez A, Dooley S, Dewidar B, Giannelli G, Ten Dijke P; IT-LIVER Consortium. TGF-β signalling and liver disease. *FEBS J* 2016; **283**: 2219-2232 [PMID: 26807763 DOI: 10.1111/febs.13665]

19 **Liu Y**, Wang Z, Wang J, Lam W, Kwong S, Li F, Friedman SL, Zhou S, Ren Q, Xu Z, Wang X, Ji L, Tang S, Zhang H, Lui EL, Ye T. A histone deacetylase inhibitor, largazole, decreases liver fibrosis and angiogenesis by inhibiting transforming growth factor-β and vascular endothelial growth factor signalling. *Liver Int* 2013; **33**: 504-515 [PMID: 23279742 DOI: 10.1111/liv.12034]

20 **Yuan S**, Dong M, Zhang H, Xu H, Wang Q, Yan C, Ye R, Jiang X, Zhou H, Chen L, Cheng J, Xie W, Jin W. Oral delivery of a Lactococcus lactis expressing extracellular TGFβR2 alleviates hepatic fibrosis. *Appl Microbiol Biotechnol* 2021; **105**: 6007-6018 [PMID: 34390354 DOI: 10.1007/s00253-021-11485-7]

21 **Haab F**, Stewart L, Dwyer P. Darifenacin, an M3 selective receptor antagonist, is an effective and well-tolerated once-daily treatment for overactive bladder. *Eur Urol* 2004; **45**: 420-9; discussion 429 [PMID: 15041104 DOI: 10.1016/j.eururo.2004.01.008]

22 **Goudie AJ**, Cooper GD, Cole JC, Sumnall HR. Cyproheptadine resembles clozapine in vivo following both acute and chronic administration in rats. *J Psychopharmacol* 2007; **21**: 179-190 [PMID: 17329298 DOI: 10.1177/0269881107067076]

23 **Haber SL**, Benson V, Buckway CJ, Gonzales JM, Romanet D, Scholes B. Lifitegrast: a novel drug for patients with dry eye disease. *Ther Adv Ophthalmol* 2019; **11**: 2515841419870366 [PMID: 31489402 DOI: 10.1177/2515841419870366]

24 **Scarlett Y**. Medical management of fecal incontinence. *Gastroenterology* 2004; **126**: S55-S63 [PMID: 14978639 DOI: 10.1053/j.gastro.2003.10.007]

25 **Patocka J**, Wu Q, Nepovimova E, Kuca K. Phenytoin - An anti-seizure drug: Overview of its chemistry, pharmacology and toxicology. *Food Chem Toxicol* 2020; **142**: 111393 [PMID: 32376339 DOI: 10.1016/j.fct.2020.111393]

26 **Silberstein SD**, Shrewsbury SB, Hoekman J. Dihydroergotamine (DHE) - Then and Now: A Narrative Review. *Headache* 2020; **60**: 40-57 [PMID: 31737909 DOI: 10.1111/head.13700]

27 **Blair HA**. Naldemedine: A Review in Opioid-Induced Constipation. *Drugs* 2019; **79**: 1241-1247 [PMID: 31267482 DOI: 10.1007/s40265-019-01160-7]

28 **Kciuk M**, Marciniak B, Kontek R. Irinotecan-Still an Important Player in Cancer Chemotherapy: A Comprehensive Overview. *Int J Mol Sci* 2020; **21** [PMID: 32664667 DOI: 10.3390/ijms21144919]

29 **Kisseleva T**, Brenner D. Molecular and cellular mechanisms of liver fibrosis and its regression. *Nat Rev Gastroenterol Hepatol* 2021; **18**: 151-166 [PMID: 33128017 DOI: 10.1038/s41575-020-00372-7]

30 **Dufton NP**, Peghaire CR, Osuna-Almagro L, Raimondi C, Kalna V, Chauhan A, Webb G, Yang Y, Birdsey GM, Lalor P, Mason JC, Adams DH, Randi AM. Dynamic regulation of canonical TGFβ signalling by endothelial transcription factor ERG protects from liver fibrogenesis. *Nat Commun* 2017; **8**: 895 [PMID: 29026072 DOI: 10.1038/s41467-017-01169-0]

31 **Ng YL**, Salim CK, Chu JJH. Drug repurposing for COVID-19: Approaches, challenges and promising candidates.

Pharmacol Ther 2021; **228**: 107930 [PMID: 34174275 DOI: 10.1016/j.pharmthera.2021.107930]

32 **Farha MA**, Brown ED. Drug repurposing for antimicrobial discovery. *Nat Microbiol* 2019; **4**: 565-577 [PMID: 30833727 DOI: 10.1038/s41564-019-0357-1]

33 **Roessler HI**, Knoers NVAM, van Haelst MM, van Haaften G. Drug Repurposing for Rare Diseases. *Trends Pharmacol Sci* 2021; **42**: 255-267 [PMID: 33563480 DOI: 10.1016/j.tips.2021.01.003]

34 **Piechal A**, Blecharz-Klin K, Joniec-Maciejak I, Pyrzanowska J, Krzysztoforska K, Mirowska-Guzel D, Widy-Tyszkiewicz E. Dihydroergotamine affects spatial behavior and neurotransmission in the central nervous system of Wistar rats. *Ann Agric Environ Med* 2021; **28**: 437-445 [PMID: 34558267 DOI: 10.26444/aaem/126020]

35 **Bernsmeier C**, van der Merwe S, Périanin A. Innate immune cells in cirrhosis. *J Hepatol* 2020; **73**: 186-201 [PMID: 32240716 DOI: 10.1016/j.jhep.2020.03.027]

36 **Campana L**, Iredale JP. Regression of Liver Fibrosis. *Semin Liver Dis* 2017; **37**: 1-10 [PMID: 28201843 DOI: 10.1055/s-0036-1597816]

37 **Cheng D**, Chai J, Wang H, Fu L, Peng S, Ni X. Hepatic macrophages: Key players in the development and progression of liver fibrosis. *Liver Int* 2021; **41**: 2279-2294 [PMID: 33966318 DOI: 10.1111/liv.14940]

38 **Binatti E**, Gerussi A, Barisani D, Invernizzi P. The Role of Macrophages in Liver Fibrosis: New Therapeutic Opportunities. *Int J Mol Sci* 2022; **23** [PMID: 35743092 DOI: 10.3390/ijms23126649]

Published by **Baishideng Publishing Group Inc**
7041 Koll Center Parkway, Suite 160, Pleasanton, CA 94566, USA
Telephone: +1-925-3991568
E-mail: bpgoffice@wjgnet.com
Help Desk: https://www.f6publishing.com/helpdesk
https://www.wjgnet.com